Wen, Z., Xu, W., Li, Q., Han, M., Tang, A., Zhang, Y., Luo, X., Shen, J., Wang, W., Li, K., Pan, Y., Zhang, L., Li, W., Collett, J. L., Zhong, B., Wang, X., Goulding, K. W. T., Zhang, F. and Liu, X. 2020. Changes of nitrogen deposition in China from 1980 to 2018. *Environment International.* 144, p. 106022. https://doi.org/10.1016/j.envint.2020.106022

Environment International 144 (2020) 106022

Contents lists available at ScienceDirect

Environment International

journal homepage: www.elsevier.com/locate/envint

Changes of nitrogen deposition in China from 1980 to 2018

Zhang Wen[a,1], Wen Xu[a,1], Qi Li[a], Mengjuan Han[a], Aohan Tang[a], Ying Zhang[a], Xiaosheng Luo[b], Jianlin Shen[c], Wei Wang[d], Kaihui Li[e], Yuepeng Pan[f], Lin Zhang[g], Wenqing Li[h], Jeffery Lee Collett Jr[i], Buqing Zhong[j], Xuemei Wang[j], Keith Goulding[k], Fusuo Zhang[a], Xuejun Liu[a,*]

[a] Key Laboratory of Plant-Soil Interactions of MOE, College of Resources and Environmental Sciences, National Academy of Agriculture Green Development, China Agricultural University, Beijing 100193, China
[b] Institute of Plant Nutrition, Resources and Environmental Sciences, Henan Academy of Agricultural Sciences, Zhengzhou 450002, China
[c] Institute of Subtropical Agriculture, Chinese Academy of Sciences, Changsha 410125, China
[d] Xizang Agriculture and Animal Husbandry College, Nyingchi, Tibet 860000, China
[e] Xinjiang Institute of Ecology and Geography, Chinese Academy of Sciences, Urumqi 830011, China
[f] State Key Laboratory of Atmospheric Boundary Layer Physics and Atmospheric Chemistry (LAPC), Institute of Atmospheric Physics, Chinese Academy of Sciences, Beijing 100029, China
[g] Laboratory for Climate and Ocean-Atmosphere Studies, Department of Atmospheric and Oceanic Sciences, School of Physics, Peking University, Beijing 100871, China
[h] Fujian Institute of Tobacco Agricultural Sciences, Fuzhou 350003, China
[i] Department of Atmospheric Science, Colorado State University, Fort Collins, CO 80523, USA
[j] Institute for Environmental and Climate Research, Jinan University, Guangzhou 510632, China
[k] The Sustainable Agricultural Sciences Department, Rothamsted Research, Harpenden AL5 2JQ, UK

ARTICLE INFO

Handling Editor: Yong-Guan Zhu

Keywords:
Reactive nitrogen
Atmospheric deposition
Ammonia
Air pollution
Emission control

ABSTRACT

China has experienced a dramatic change in atmospheric reactive nitrogen (Nr) emissions over the past four decades. However, it remains unclear how nitrogen (N) deposition has responded to increases and/or decreases in Nr emissions. This study quantitatively assesses temporal and spatial variations in measurements of bulk and calculated dry N deposition in China from 1980 to 2018. A long-term database (1980–2018) shows that bulk N deposition peaked in around 2000, and had declined by 45% by 2016–2018. Recent bulk and dry N deposition (based on monitoring from 2011 to 2018) decreased from 2011 to 2018, with current average values of 19.4 ± 0.8 and 20.6 ± 0.4 kg N ha^{-1} yr^{-1}, respectively. Oxidized N deposition, especially dry deposition, decreased after 2010 due to NO_x emission controls. In contrast, reduced N deposition was approximately constant, with reductions in bulk NH_4^+-N deposition offset by a continuous increase in dry NH_3 deposition. Elevated NH_3 concentrations were found at nationwide monitoring sites even at urban sites, suggesting a strong influence of both agricultural and non-agricultural sources. Current emission controls are reducing Nr emissions and deposition but further mitigation measures are needed, especially of NH_3, built on broader regional emission control strategies.

1. Introduction

Over the last century humans have at least doubled the amount of reactive nitrogen (Nr) compounds in the biosphere due to increased agricultural and industrial activities (Galloway et al., 2004). Much of this anthropogenic nitrogen (N) enters natural and semi-natural ecosystems via atmospheric deposition, which is an important component of N cycling (Galloway et al., 2008). Excess N deposition can cause adverse ecological effects in terrestrial and aquatic environments, including soil acidification (Johnson et al., 2018), eutrophication of coastal waters and lakes (Zhan et al., 2017) and reductions in biodiversity (Midolo et al., 2019; Nair et al., 2016). Over the last 30 years, the effectiveness of Nr emission controls by governments has been demonstrated in some regions (e.g., Europe, North America), as proven by decreasing atmospheric Nr concentrations and deposition (Ackerman et al., 2019; Li et al., 2016). In contrast, N deposition continues to increase, or at least not decrease rapidly, particularly in East Asia and most parts of India (Gupta et al., 2003; Xu et al., 2015).

* Corresponding author.
E-mail address: liu310@cau.edu.cn (X. Liu).
[1] Co-first authors.

https://doi.org/10.1016/j.envint.2020.106022
Received 9 March 2020; Received in revised form 30 May 2020; Accepted 28 July 2020

China, with the largest area and population in East Asia, has witnessed severe air pollution problems over recent decades (Huang et al., 2014). Concentrations of particulate matter (PM) and many gaseous pollutants have increased significantly due to rapid industrialization, urbanization, and intensified agricultural production (An et al., 2019). The combustion of fossil fuels, increased more than 6 times from 1980 to 2018 (China statistical yearbook, http://www.stats.gov.cn/tjsj/ndsj/), and is the major contributor to NO_x in the atmosphere. Synthetic fertilizer production represents an important source of NH_3 emissions, having increased threefold during the past three decades, from approximately 10 million tons in 1980 to 33 million tons in 2010 (Liu et al., 2013). China has experienced a growing public awareness of air pollution in recent years; to alleviate this and improve environmental quality, a series of government laws, regulations, and standards have been enacted (Zheng et al., 2018). One example is the setting of more ambitious goals to reduce annual SO_2 and NO_x emissions by 15% and 10%, respectively, by 2021 from their 2016 levels. This follows successfully achieving binding goals for the 11th Five-Year-Plan (FYP, 2006–2010) of 8% reductions for SO_2 emissions, and the 12th FYP (2011–2015) of a further 8% and 10% for SO_2 and NO_x emissions, respectively. Previous efforts have been designed to reduce acid precursor emissions. Reductions of alkaline gas emissions, such as NH_3, a critical influencing factor for secondary inorganic aerosol formation (which accounts for 40–57% of $PM_{2.5}$ in eastern China (Huang et al., 2014; Yang et al., 2011), the most damaging air pollutant to human health (Chen et al., 2017), have not been a priority. Evidence from emission inventory studies confirms that total NH_3 emissions in China remain high (Huang et al., 2012; Kang et al., 2016). Zhang et al. (2017) reported that total NH_3 emissions in China could have been substantially underestimated in previous studies, and were 15.6 Tg N yr^{-1} rather than the previously estimated 12.1 Tg N yr^{-1} during 2000–2015.

China is one of three global hotspots for N deposition (Vet et al., 2014). A meta-analysis of historic data by Liu et al. (2013) showed that bulk N deposition (wet plus a certain unknown fraction of dry deposition) in China increased from 13.2 kg N ha^{-1} yr^{-1} in the 1980s to 21.1 kg N ha^{-1} yr^{-1} in the 2000s. Yu et al. (2019) further quantified trends in atmospheric wet and dry N deposition and reported that total N deposition stabilized after 2005, and estimated total deposition as 20.4 ± 2.6 kg N ha^{-1} yr^{-1} in 2011–2015. However, the main weakness of their study was the large uncertainty of earlier dry N deposition, which was obtained by empirical modeling. Meanwhile, Yu et al. (2019) only considered the period up to 2015, thereby missing main impact from recent major emission control measures of air pollutants taken at a national scale (e.g. the effect of the ten air pollution control regulations enacted after June 2013).

Thus, the objectives of this study were to: (1) examine long-term trends of N deposition via different pathways (dry and bulk N deposition) and in various chemical forms (reduced and oxidized N) in China from 1980 to 2018; (2) explore the relationship between N deposition and emissions to check any potential delay in the response of N deposition to Nr emission reductions. N deposition was quantified in two ways. First, a long-term database of bulk deposition in China from 1980 to 2018 was established using data from published papers. Second, a database of dry and bulk deposition of various Nr species after 2010 was obtained from a nationwide monitoring network. The two databases jointly reveal temporal and spatial variations in N deposition across China over a period of almost four decades. The results will help identify effective and feasible measures to decrease N deposition to sensitive ecosystems and will also provide useful guidance regarding Nr pollution control in China and other rapidly developing countries.

2. Methods

2.1. Long-term national datasets of bulk N deposition

Data with high spatial and temporal resolution are necessary for analyzing the regional characteristics of bulk N deposition in China. Bulk N deposition data were obtained from articles published after 1980, using "precipitation" and "atmospheric nitrogen deposition" as keywords (Table S1). Each dataset included event-based precipitation measurements together with Nr species concentrations, with a minimum sampling record of one year. The datasets included information on the monitoring site (including province, location, latitude, and longitude), the monitoring period, rainfall, concentrations and deposition fluxes of NH_4^+-N, NO_3^--N, and DIN (dissolved inorganic nitrogen, the sum of NH_4^+-N and NO_3^--N).

Based on these criteria, a total of 951 yearly data points were obtained from 1980 to 2018 (Fig. S1). To better understand the spatial and temporal distribution of bulk N deposition in China, the country was divided into six regions based on socioeconomic development and geographical information: North China, Northwest China, Northeast China, Southeast China, Southwest China, and the Qinghai-Tibet Plateau.

2.2. Monitoring networks of bulk and dry N deposition

A Nationwide Nitrogen Deposition Monitoring Network (NNDMN) covered sixty-six *in situ* monitoring sites across China (Fig. S1). This network, established and operated by China Agricultural University, quantifies bulk and dry deposition of major Nr species in air (as gaseous and particulate forms) and in precipitation. It has become an important long-term monitoring platform for the region. In order to ensure the representativeness of the sampling sites, quantification of N deposition was mostly conducted in eastern China, with its high emissions of NH_3 and NO_x, and fewer sampling sites in western China with less anthropogenic activity. The 66 sites cover major land use types, including urban, rural (cropland), and background regions (coastal, forest, and grassland). More details on each site can be found in Table S2.

Measurements at all NNDMN sites were conducted from 2011 to 2018. Ambient gaseous (NH_3 and HNO_3), and particulate (pNH_4^+ and pNO_3^-) Nr samples were collected with active DELTA (Denuder for Long-Term Atmospheric sampling, Center for Ecology and Hydrology, Edinburgh, UK) samplers, while NO_2 samples were collected with Gradko passive diffusion tubes (Gradko International Limited, UK) deployed in duplicate or triplicate. NH_3 was also sampled using an ALPHA passive sampler (Adapted Low-cost High Absorption, Center for Ecology and Hydrology, Edinburgh, UK) at all monitoring sites for double insurance. In total, there were approximately 30,000 samples collected over the 8 years to estimate dry deposition fluxes.

Precipitation samples were collected in rain gauges (SDM6, Tianjin Weather Equipment Inc., China), which were placed on open flat land with no obstacles or distinct nearby sources of pollution. An anti-bird device was installed on the rain gauges to avoid contamination by bird droppings. Approximately 2000 precipitation samples were collected by the network each year. More detailed information on sample processing can be found in Text S1. Quality control procedures were applied during all analytical processes as described by Xu et al. (2019a).

Direct methods for measuring dry deposition (e.g., eddy correlation; chambers) are difficult and expensive. The inferential method is an indirect method that estimates dry deposition fluxes of Nr species using a combination of ambient Nr concentrations and their dry deposition velocities (Fowler et al., 1990). Dry N deposition was calculated as the product of the measured Nr concentration and simulated deposition velocity (V_d). The GEOS-Chem chemical transport model (CTM; http://geos-chem.org) was used to simulate the V_d values of five Nr species every hour at each monitoring site from 2011 to 2018. Hourly V_d values were averaged to obtain a monthly V_d, which was multiplied by the monthly species concentration to estimate the dry deposition flux. The details of inputs of the model, including meteorological data, domain, resolution, and land use type are presented in Text S2. The V_d values of gaseous NH_3, NO_2, HNO_3 and particulate NH_4^+ and NO_3^- all showed no significant differences from 2011 to 2018 ($p > 0.05$) (Fig. S2).

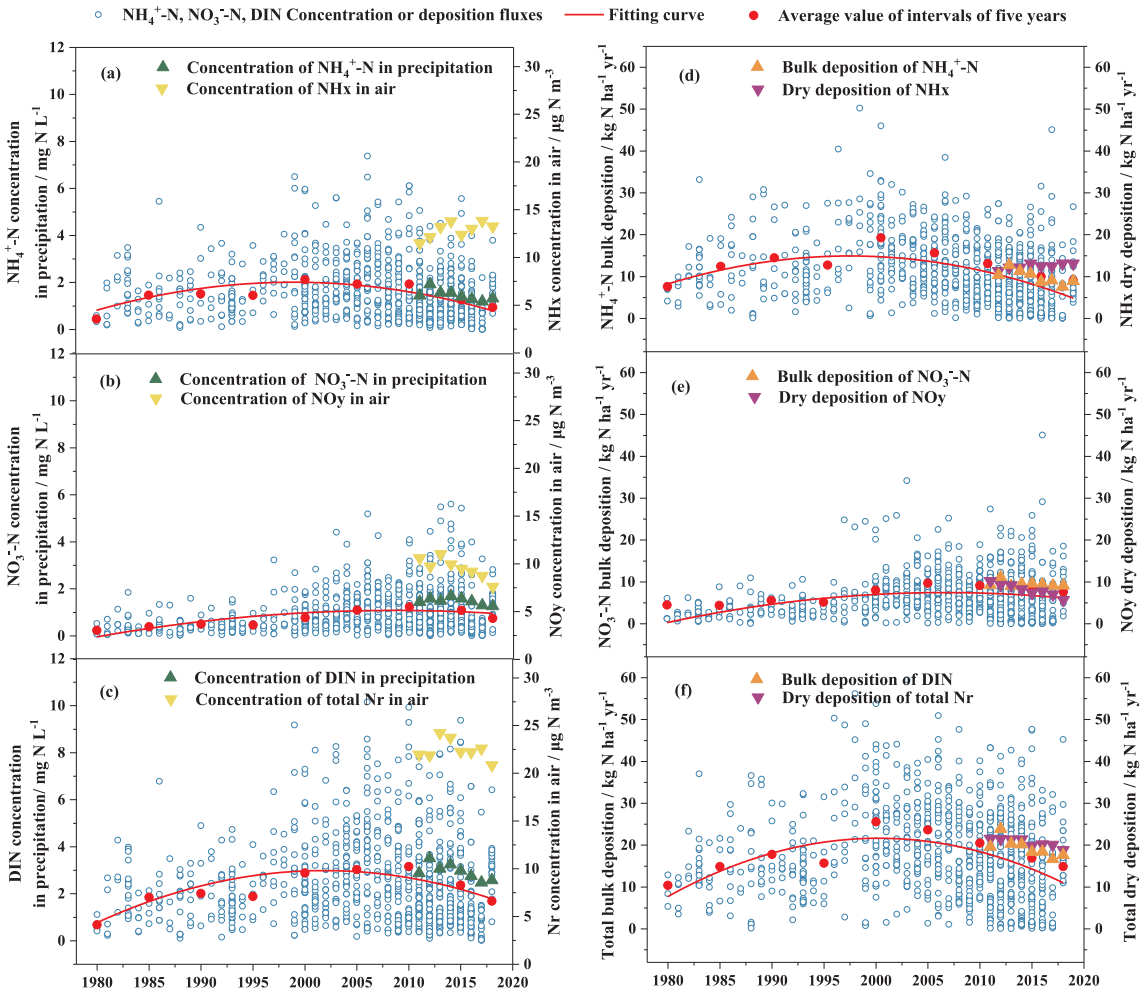

Fig. 1. Annual mean concentrations (a, b, c) and deposition (d, e, f) of inorganic N in precipitation and reduced and oxidized N species in air derived from two complementary databases: (1) published long-term data of bulk N deposition covering 1980–2018, and (2) short-term NNDMN-based bulk and dry N deposition fluxes (calculated on the bases of measured N_r concentrations and deposition velocities) from 2011 to 2018. For the long-term data, the blue open circles represent annual average concentrations of inorganic N species in precipitation: NH_4^+-N (a), NO_3^--N (b), DIN (c) and bulk N deposition: NH_4^+-N (d), NO_3^--N (e), DIN (f); the red curve shows the trends in inorganic N concentrations in precipitation and bulk deposition, while the red dots represent the 5-year average inorganic N concentration and bulk deposition, except in 1980 (only that year's average) and in 2018 (the average of 2016–2018) (N = 951). For the short-term data, the green triangles represent the concentrations of inorganic N species in precipitation: NH_4^+-N (a), NO_3^--N (b), DIN (c) and orange triangles represent bulk deposition: NH_4^+-N (d), NO_3^--N (e), DIN (f); the yellow triangles represent the concentrations of Nr species in air: NH_x (gaseous NH_3 plus particulate NH_4^+) (a), NO_y (gaseous HNO_3, NO_2 plus particulate NO_3^-) (b), Total Nr (NH_x plus NO_y) (c) and the purple triangles represent dry deposition: NH_x (d), NO_y (e), Total Nr (f), respectively. (For interpretation of the references to colour in this figure legend, the reader is referred to the web version of this article.)

Therefore, calculated trends in dry deposition are not a function of V_d, but follow the measured Nr concentrations in air.

3. Results and discussion

3.1. Interannual variation of N deposition across China

The long-term trend over a period of 39 years shows that bulk N deposition across China reached a maximum around 2000 and then began to gradually decline (Fig. 1). Deposition of DIN (the sum of NH_4^+-N and NO_3^--N) in precipitation increased from 8.88 ± 2.20 kg N ha^{-1} yr^{-1} (mean ± standard error) in 1980 to 24.5 ± 1.47 kg N ha^{-1} yr^{-1} during 1996–2000, and afterward decreased to 13.5 ± 1.43 kg N ha^{-1} in 2016–2018 (Fig. 1f), mirroring trends in NH_4^+-N rather than NO_3^--N, the deposition of which remained relatively constant after 2000 (Fig. 1d, e). Not surprisingly, trends in the concentrations of inorganic N in precipitation were similar to those of deposition (Fig. 1a, b, c). That the observed decline in bulk DIN deposition is driven by changes in bulk NH_4^+-N deposition is consistent with evidence from Yu et al. (2019), that total N deposition began to stabilize around 2005 due to a gradual decline in wet NH_4^+-N deposition.

The monitoring network recorded an average annual concentration of DIN of 2.94 ± 0.12 mg N L^{-1} during 2011–2018 (Fig. 1c). Consistent with the long-term trends in bulk deposition, the average DIN deposition measured by the network was 19.4 ± 0.78 kg N ha^{-1} yr^{-1}, showing a decline (p = 0.01) over the monitoring period (Fig. 1f). As shown in previous studies (Xu et al., 2015), dry N deposition is as important as bulk N deposition at the national scale, so neglecting dry deposition can result in a substantial underestimation of the total N deposition flux. The total Nr concentrations in air (the sum of NH_3, HNO_3, NO_2, pNH_4^+, and pNO_3^-) averaged 22.5 ± 0.38 μg N m^{-3} (Fig. 1c), and the annual dry N deposition showed a minor decrease from 2011 to 2018, with an overall average value of 20.6 ± 0.35 kg N ha^{-1} yr^{-1} (Fig. 1f). Total N deposition (bulk plus dry deposition) declined significantly (p < 0.01) from 2011 to 2014 (average 42.2 ± 0.98 kg N ha^{-1} yr^{-1}) to 37.5 ± 0.55 kg N ha^{-1} yr^{-1} in 2015–2018.

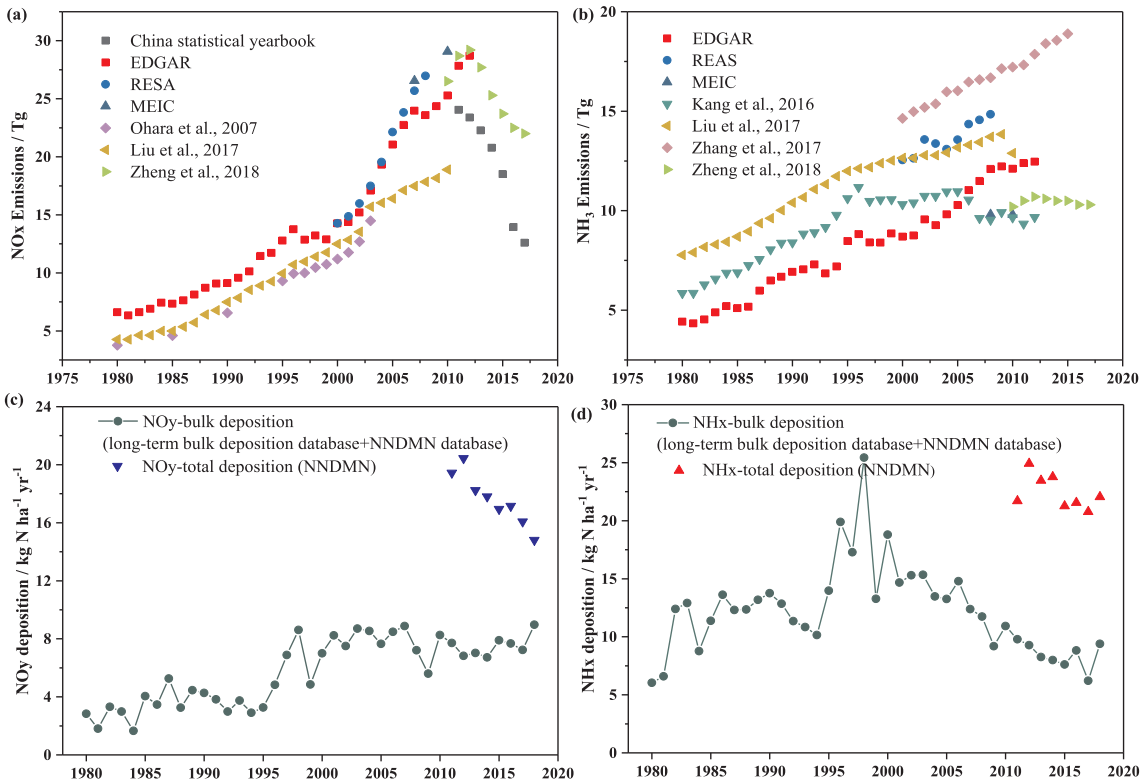

Fig. 2. NO_x (a) and NH_3 (b) emissions from emission inventories and the observed deposition of oxidized N (NO_y) (c) and reduced N (NH_x) (d) across China over the past four decades. In panels (c) and (d), the green lines represent results from the long-term bulk deposition database and the NNDMN database, and the blue and red scatter points represent observed total deposition. NO_x and NH_3 emissions data were obtained from the China statistical yearbook (http://www.stats.gov.cn/), EDGAR (https://edgar.jrc.ec.europa.eu/), RESA (http://www.nies.go.jp/REAS/), MEIC (http://www.meicmodel.org/), and publications (Ohara et al., 2007; Liu et al., 2017; Kang et al., 2016; Zhang et al., 2017; Zheng et al., 2018). (For interpretation of the references to colour in this figure legend, the reader is referred to the web version of this article.)

Anthropogenic emissions of NO_x ($NO + NO_2$) and NH_3 show a marked increase from 1980 to 2010, after which NH_3 emissions continued to increase while NO_x emissions began to decrease, reflecting measures taken to reduce NO_x emissions (Fig. 2a, b). Correspondingly, total oxidized N deposition (NO_3^--N in bulk deposition plus HNO_3, NO_2, and pNO_3^- in dry deposition) has decreased in recent years, while the total amount of reduced N deposition (NH_4^+-N in bulk deposition plus NH_3 and pNH_4^+ in dry deposition) has remained stable, despite a decline in bulk NH_4^+-N deposition (Fig. 2c, d).

China has faced a series of socio-economic changes over the past four decades, during which urbanization increased from 19.4% in 1980 to 59.6% in 2018, along with a dramatic 7.6-fold increase in energy consumption (Fig. S3). Consequently, the country has experienced frequent and severe air pollution episodes over the past decade (Cui et al., 2016). To improve air quality, protect ecosystems and ensure ecosystem service function, the Chinese government has adopted stringent control measures to reduce emissions and deposition fluxes of air pollutants (e.g., SO_2, NO_x, particles) from manufacturing, power plants, and transportation, such as widespread implementation of flue gas desulfurization, mandatory transformation of energy structures, and the active promotion of clean energy vehicles (Fig. S4). Our findings reflect the positive effects of the implementation of such measures on the mitigation of atmospheric Nr pollution in China.

From an eco-environmental protection perspective, mitigation of N deposition is undoubtedly beneficial in reducing potential acidification and eutrophication risks in natural and semi-natural ecosystems. However, we found the total potential acidifying N deposition fluxes averaged 40.0 ± 1.06 kg N ha^{-1} yr^{-1} during 2011 and 2018, much higher than the critical loads (< 28 kg N ha^{-1} yr^{-1}) for acidification in most areas in China, even without considering atmospheric sulfur deposition. The total potential acidifying N deposition declined by 11% in 2018 compared with 2011. SO_2 emission abatement in China has been reported to have had a positive effect on the recovery of acidified soil and water bodies (Duan et al., 2013). Benefits may also be anticipated from a decline in N deposition as it has been found that N deposition can acidify soils in tropical ecosystems, temperate forests and waters (Bonten et al., 2016; Oulehle et al., 2011; Lu et al., 2014). Schmitz et al. (2018) reported a potential response in soil solution and foliage concentrations to decreasing N deposition for Europe's forests.

3.2. A shift in oxidized and reduced N deposition

Bulk NH_4^+-N deposition reached a peak in 1996–2000 (18.0 ± 1.15 kg N ha^{-1} yr^{-1}), and had decreased by more than half by 2016–2018 (7.55 ± 0.82 kg N ha^{-1} yr^{-1}) (Fig. 1d). In contrast, the change point for bulk NO_3^--N deposition occurred in 2001–2005 (8.16 ± 0.42 kg N ha^{-1} yr^{-1}) with subsequent values being approximately constant (Fig. 1e). Thus, the NH_4^+-N/NO_3^--N ratio increased in the early 1980s, then decreased significantly from 1984 to 2018 ($p < 0.01$) at a rate of −0.17 yr^{-1} (Fig. 3a). The consequence is that bulk N deposition changed from being NH_4^+-N dominated to NH_4^+- N and NO_3^--N being equally important (Fig. S3). A similar ratio of reduced to oxidized N in bulk deposition was observed in the NNDMN data (Fig. 3c). Dry NH_x deposition (NH_3 and pNH_4^+ in dry deposition) increased from 2011 to 2018 at a rate of 0.23 kg N ha^{-1} yr^{-1} ($p < 0.05$), while dry NO_y deposition (HNO_3, NO_2, and pNO_3^- in dry deposition) markedly declined at a rate of −0.57 kg N ha^{-1} yr^{-1} ($p < 0.01$) (Fig. 1d, e), leading to a significant increase in the ratio of reduced to oxidized N in dry deposition (Fig. 3b). The observed decrease in bulk NH_x deposition (NH_4^+-N in bulk deposition) was offset

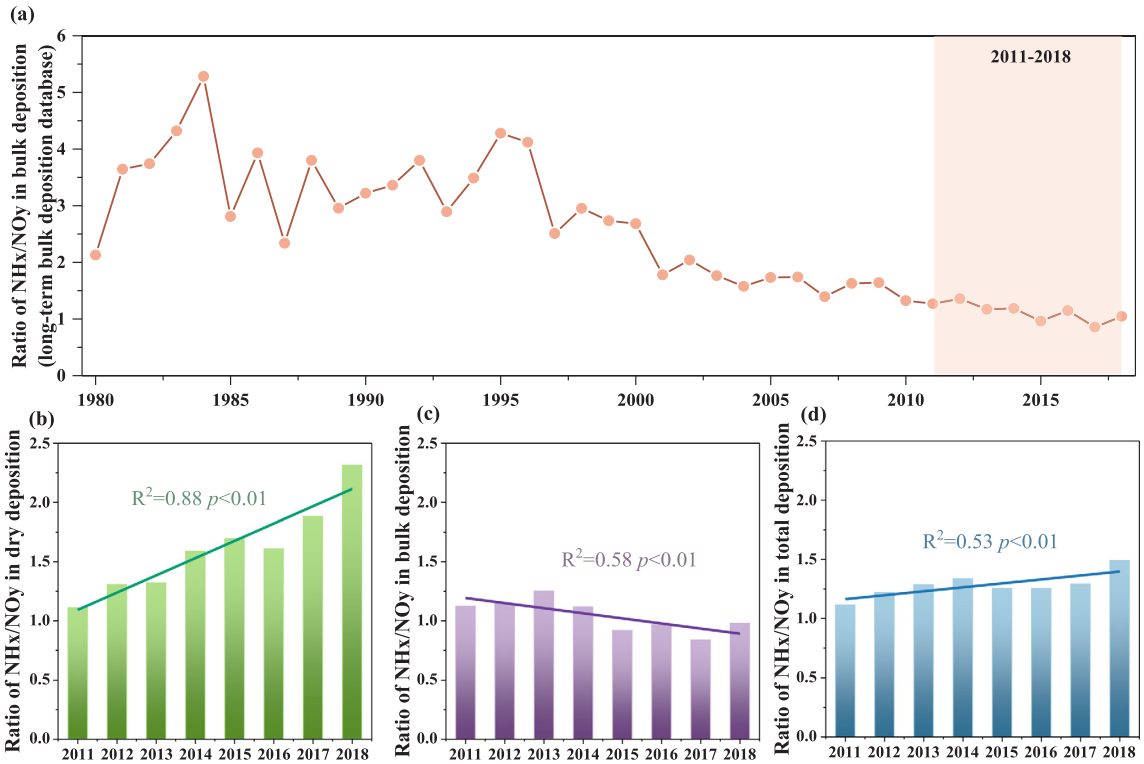

Fig. 3. Annual variations in the ratio of reduced N (NH_x) to oxidized N (NO_y) species in long-term bulk deposition (a), and dry (b), bulk (c), and total deposition (d) measured in the short-term monitoring network in China. Green, purple and blue lines represent linear fits for dry, bulk, and total N deposition, respectively. (For interpretation of the references to colour in this figure legend, the reader is referred to the web version of this article.)

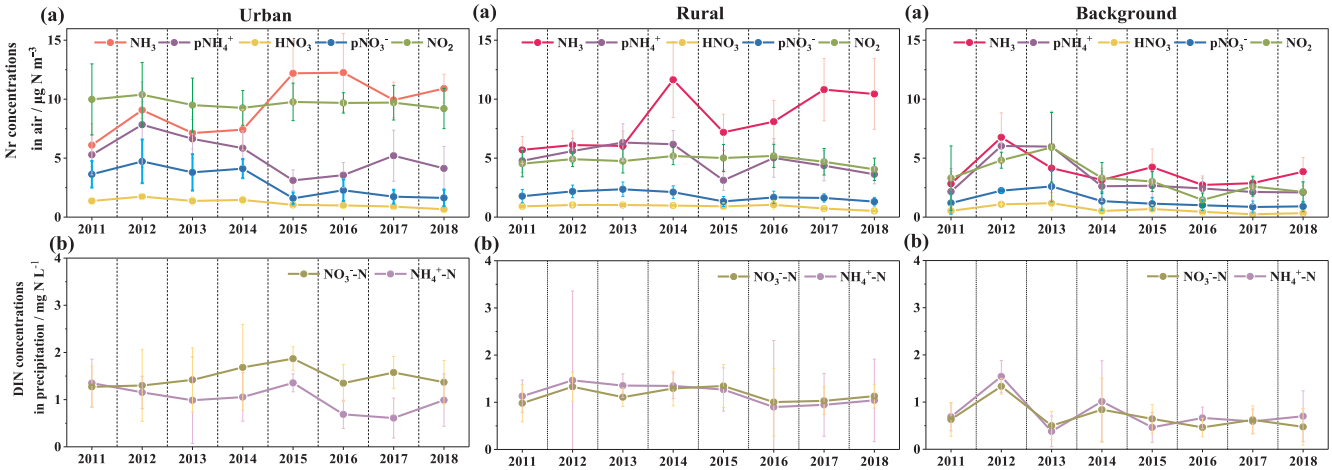

Fig. 4. Annual mean concentrations of Nr species in urban (a), rural (b) and background (c) land use types from 2011 to 2018. Top: Nr concentrations in the air; bottom: Nr concentrations in precipitation. Light colored lines represent standard errors.

by an increase in dry NH_x deposition, which resulted in an approximately constant level of total NH_x deposition from 2011 to 2018. In contrast, annual dry NO_y deposition significantly declined, while annual bulk NO_y deposition (NO_3^--N in bulk deposition) remained relatively constant, resulting in a decrease in total NO_y deposition (Fig. 3d). The implementations of strict control measures (Fig. S4) have successfully reduced NO_x emissions over recent years (Fig. 2a, c) as seen in the observed decrease in oxidized N deposition.

A substantial reduction in atmospheric SO_2 concentrations has been observed since 2005 (Fig. S5). A rapid reduction of SO_2 can significantly reduce the formation of ammonium sulfate ($(NH_4)_2SO_4$) and then increase the proportions of gas-phase NH_3 (Bleeker et al., 2009; Sutton et al., 2003). The increased NH_3 concentration can be attributed to the release of NH_4^+ from the aerosol phase as a semi-volatile property of ammonium nitrate (NH_4NO_3) and associated aerosol water. Thus, a possible explanation of decreased NH_4^+ bulk deposition is that more NH_3 is partitioned to the gaseous phase, reducing the NH_4^+ concentration in the particle-phase and in precipitation. Lachatre et al. (2019) showed that SO_2 and NO_x emissions in China between 2011 and 2015 were reduced by 37.5% and 21%, respectively, in agreement with an increase in gaseous NH_3 concentrations by as much as 49%. This, in turn, led to an increase in gaseous NH_3 concentrations by as much as 49% from 2011 to 2015, similar to the 48% increase in NH_3 concentrations during the same period across all sites in this study. According to recent research, the enhanced atmospheric NH_3 concentration over China between 2002 and 2016 mainly resulted from increased fertilizer use and increasing temperatures (Warner et al., 2016), together with substantial reductions in SO_2 and NO_x emissions since 2011

(Chen et al., 2020). Response times between decreases of NO_x emissions and NO_y wet deposition were associated with the reduction rates of NO_x emissions, and the atmospheric acidity and humidity, which determine the gas-aerosol partitioning of NO_3^- (Tan et al., 2018). Therefore, the effectiveness of NO_x emissions control may first be reflected in the gaseous concentration, then the aerosol or precipitation.

During 2011–2018, the annual mean ambient NO_y concentrations (the sum of NO_2, HNO_3, and pNO_3^-) were higher at urban sites (13.6 ± 3.04 μg N m^{-3}) than rural (7.49 ± 1.58 μg N m^{-3}) and background sites (5.22 ± 2.19 μg N m^{-3}) (Fig. 4). NO_y concentrations decreased by 23.2%, 20.9%, and 32.9% at urban, rural, and background sites, respectively, in 2018 compared to 2011, further demonstrating the effectiveness of NO_x emission controls across China. The annual mean oxidized and reduced species concentrations in precipitation showed different patterns across the three land-use types, as shown in Fig. 4. NO_3^--N deposition was the main component in bulk N deposition at urban sites, while equal contributions from NH_4^+-N and NO_3^--N were found at rural and background sites.

China is one of the largest grain and meat producers in the world, so agricultural NH_3 emissions (mainly from fertilization and livestock manure) have substantially increased over the last four decades (Kang et al., 2016). Annual NH_3 concentrations at rural and urban sites increased by approximately 83% and 78%, respectively, from 2011 to 2018, whereas no clear trend was found at background sites. Furthermore, a substantial increase in the ratio of $NH_3/(NH_3 + pNH_4^+)$ at rates of 4.41% yr^{-1} and 5.25% yr^{-1} was observed at urban and rural sites, respectively, indicating that the atmospheric environment of China is increasingly NH_3-rich.

The average NH_3 concentration at rural monitoring sites (8.25 ± 1.97 μg N m^{-3}) was comparable to that at urban monitoring sites (9.37 ± 1.80 μg N m^{-3}). However, sources of NH_3 in urban areas are complex. Atmospheric NH_3 is a short-lived Nr species and mainly locally deposited. For example, Xu et al. (2014) have found a 64% reduction in ambient NH_3 concentration at 650 m distance from the source. In addition to agricultural sources, non-agricultural sources of NH_3 emissions (e.g., vehicles and coal combustion) have attracted increasing attention because of their potential to form secondary inorganic aerosols, especially in urban areas (Huang et al., 2018; Pan et al., 2016). A high-resolution NH_3 emission inventory for combustion and industrial sources showed that the emission density of NH_3 in urban areas was an order of magnitude higher than in rural areas (Meng et al., 2017). Reducing NH_3 emissions by improved N management practices (e.g. Ju et al., 2009; Sha et al., 2020) should be a priority in curbing N deposition in China.

3.3. Spatial distribution of DIN in precipitation and Nr pollution in air

Fig. 5 shows the bulk and dry deposition in regions of China; both show large spatial variability. Total N deposition followed the order: North China (NC) > Southwest China (SW) and Southeast China (SE) > Northeast China (NE) > Northwest China (NW) > Qinghai-Tibet Plateau (TP). North China has the highest dry N deposition (27.8 ± 0.57 kg N ha^{-1} yr^{-1}) and total N deposition (47.4 ± 1.90 kg N ha^{-1} yr^{-1}), mainly due to differences in regional emissions of NH_3 and NO_x (Xu et al., 2015). The Qinghai-Tibet Plateau has the lowest total N deposition (12.3 ± 2.79 kg N ha^{-1} yr^{-1}), consistent with its limited anthropogenic disturbance. Earlier, Pan et al. (2012) reported that total N deposition in NC reached 60.6 kg N ha^{-1} yr^{-1} from 2007 to 2010, 60% of which was comprised of dry-deposited forms. Total N deposition in NC began to decrease from 2011 to 2018, mainly due to a decline in bulk deposition and the stabilization of dry deposition (Fig. S6).

Meteorological and geographical conditions significantly affect N deposition. High bulk N deposition is observed not only in NC, but also in SE (21.8 ± 1.23 kg N ha^{-1} yr^{-1}) and SW (21.9 ± 1.62 kg N ha^{-1} yr^{-1}), a pattern also observed in long-term bulk deposition data (Fig. 5b and S7). Precipitation amounts were positively and significantly correlated ($p < 0.01$) with bulk N deposition, and negatively correlated ($p < 0.01$) with DIN concentrations (Fig. S8). Analyzing 39 years of data, the average annual precipitation in NC was 531.7 ± 10.9 mm, 1441.5 ± 27.4 mm in SE, and 1063.0 ± 29.6 mm in SW. Higher amounts in southern China contributed to the high bulk deposition in SE and SW. Rain generally efficiently removes water-soluble gaseous pollutants and large aerosol particles from the atmosphere (Al-Khashman, 2005; Xu et al., 2017). In contrast, in regions with severe air pollution and/or less precipitation, dry deposition is often the dominant deposition pathway. Bulk deposition was the main form of deposition in southern areas of China, while dry deposition was predominant in drier northern China.

As shown in Table 1, China has experienced enhanced N deposition at background sites compared with such sites at international monitoring locations observed by NADP, EMEP, and Japan's EANET network, indicating that local atmospheric N deposition levels are affected by regional Nr emissions. Current annual dry and bulk N deposition, estimated in this study (20.6 ± 0.4 and 19.4 ± 0.8 kg N ha^{-1} yr^{-1}), were both approximately twice the corresponding values (10.3 ± 1.5 and 10.1 ± 1.2 kg N ha^{-1} yr^{-1}, respectively) reported by Yu et al. (2019) for the 2011–2015 period. This is not surprising, mainly because the national magnitudes of dry and wet N deposition from the study of Yu et al. (2019) were estimated based on a Kriging interpolation technique, rather than arithmetic averaging used in this study. As reported by Zhao et al. (2017), China's domestic anthropogenic sources contribute 86% of the total deposition, foreign anthropogenic sources 7% and natural sources 7%. This suggests that emission reductions should be planned at large scales. In the United States, insight into the balance between oxidized and reduced N revealed a significant shift

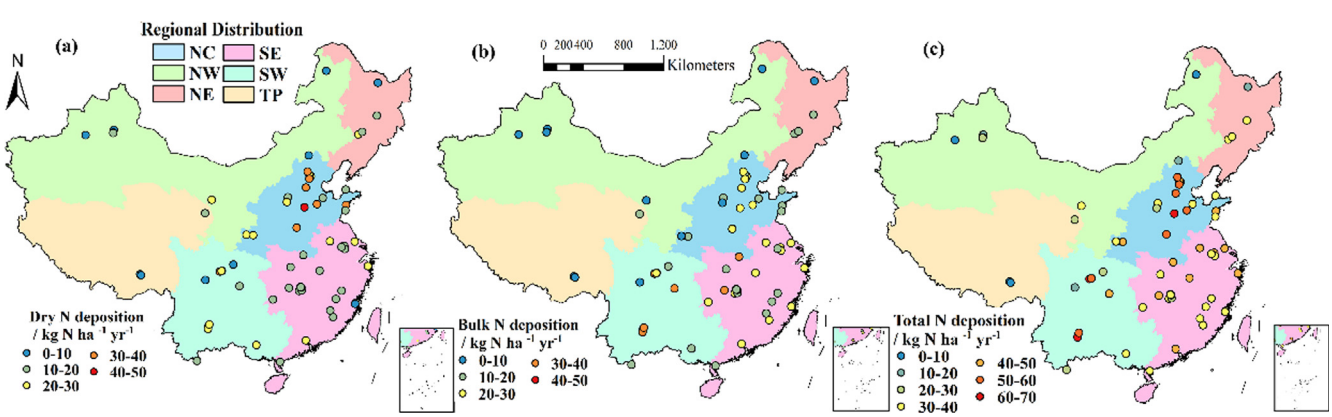

Fig. 5. Maps of dry deposition (a), bulk deposition (b) and total deposition (c) created from the NNDMN monitoring sites in North China (NC), Northwest (NW), Northeast (NE), Southeast (SE), Southwest (SW) and Qinghai-Tibet Plateau (TP) of China, respectively.

Table 1
Comparison of total N deposition (kg N ha^{-1} yr^{-1}) between NNDMN (background) and other regional monitoring networks (NANET-Japan, CASTNET, EMEP).

Network	[a]EANET-Japan			[b]CASTNET			[c]EMEP			NNDMN (background)		
Number of sites	10			264			2447 girds (0.5∘ × 0.5∘)			10		
Observation period	2000–2017			2000–2017			2003–2007			2011–2018		
N deposition	wet	dry	total	wet	dry	total	wet	dry	total	wet/bulk	dry	total
	6.1	4.9	11.0	3.6	4.5	8.1	3.9	4.8	8.7	12.4	11.2	23.6

[a] The EANET-Japan data are sourced from https://www.eanet.asia/.
[b] The CASNET data are available online (http://www.epa.gov/castnet/).
[c] The EMEP data are sourced from EMEP website, in which the dry and wet deposition amounts at each grid covering 27 EMEP countries were estimated by the unified EMEP models.

from NO_3-dominated to NH_4-dominated conditions. Reduced N deposition, which is not regulated, accounted for 65% of N deposition from 2011 to 2013 (Du et al., 2014; Li et al., 2016). This is similar to our NNDMN results from 2011 to 2018, which showed that reduced N contributed an average of 56% to the total N deposition amount and continues to increase.

3.4. Policy implications

The long-term bulk deposition records show a downward trend since 1998; measured short-term bulk and calculated dry deposition continuously decreased from 2011 to 2018, caused by adjustments of energy production structures and strong support of environmental policies in China. Total potential acidifying N deposition declined by 11% and should result in a degree of recovery of acidified soil and water bodies. However, when compared with the critical load, the ecological impact of atmospheric N deposition is still much too high. After completion of the "Action Plan for Prevention and Control of Air Pollution" (2013–2017), the Chinese government has announced plans to roll out a three-year plan (2018–2020) to ensure even greater reductions in air pollution. Many positive policy and practical changes are taking place, so further evaluation using field measurements of Nr deposition (or emission) fluxes in typical ecosystems (e.g., cropland, forest, grassland) over a longer period is recommended. The trend in Nr concentrations and deposition can also be quantified using an atmospheric model based on long-term emission inventories (e.g. Kang et al., 2016; Crippa et al., 2020). The observations presented in this study can be valuable for evaluating the performance of atmospheric models and improving the accuracy of emission inventories. Future work will focus on quantifying the trends in the concentrations/deposition fluxes of atmospheric reactive N by combing atmospheric chemistry model simulations and in-situ observations (More details of uncertainty in dry and wet deposition are presented in Text S3).

Reduced N deposition, which stems from the mostly uncontrolled NH_3 emissions, has become the dominant form of N deposition. While some decrease has been observed in the bulk deposition of NH_4^+, dry NH_3 deposition has dramatically increased at a rate of 0.31 kg N ha^{-1} yr^{-1}. Furthermore, there were no significant differences in measured NH_3 concentrations between urban and rural monitoring sites, indicating that non-agricultural emissions of NH_3 need urgent attention. Bulk and dry deposition fluxes of oxidized N are expected to continue to decrease in the future as China's government continues to reduce SO_2 and NO_x emissions by implementing strict emission reduction measures, such as upgrading coal-burning equipment, encouraging the use of desulfurization and denitration technologies, promoting the development of clean and renewable energy, controlling pollution sources, and restricting motor vehicle use. From the experience of air quality improvements in Europe and the United States, NH_3 emissions present a serious environmental issue with the sharp reduction of acidic precursors (Backes et al., 2016). Optimizing fertilizer application by improving application methods and utilization rates and their uptake must be a priority in China (Zhang et al., 2019), which is also key to establishing green eco-environment (Liu et al., 2020). Livestock manure management, including reductions in the crude protein content of feed and acidifying slurry, are strategies that could consistently reduce NH_3 emissions (Hou et al., 2015). Xu et al. (2019b) showed, in simulations, that better livestock manure management during winter in northern China could reduce NH_3 concentrations by 40%, contributing to a reduction of 37% for pNO_3^- during a severe haze episode. At the same time, accurate identification and effective control of non-agricultural NH_3 sources are essential, especially for urban areas (Zhang et al., 2020). Recent simulations have shown that 50% NH_3 emission reductions, together with 15% reductions in SO_2 and NO_x emissions, could mitigate $PM_{2.5}$ concentrations by 11–17% and N deposition by 33%, but significantly increase the acidity of precipitation (Liu et al., 2019). Research is needed to identify the sources of different Nr components in deposition to provide region-specific strategies for the prevention and control of multiple air pollutants. An effective emission reduction plan should be formulated by combining the effects of different land use types in different regions on N deposition, according to the most appropriate economic-ecological effects. In other words, more attention not only should be paid to the control of NO_x emissions from China's core urban agglomerations or industrial cities, but to the control of NH_3 emissions from cropland and livestock production dominated agricultural areas. In summary, emission reduction policies, based on sound science, are needed. This paper provides basic information for future environmental quality governance.

CRediT authorship contribution statement

Zhang Wen: Investigation, Formal analysis, Visualization, Writing - original draft. **Wen Xu:** Investigation, Formal analysis, Visualization, Writing - original draft. **Qi Li:** . **Mengjuan Han:** . **Aohan Tang:** . **Ying Zhang:** . **Xiaosheng Luo:** . **Jianlin Shen:** . **Wei Wang:** Investigation, Formal analysis. **Kaihui Li:** Investigation, Formal analysis. **Yuepeng Pan:** Investigation, Formal analysis. **Lin Zhang:** Methodology, Software, Writing - review & editing. **Wenqing Li:** Investigation, Formal analysis. **Jeffery Lee Collett:** Writing - review & editing. **Buqing Zhong:** Investigation, Formal analysis. **Xuemei Wang:** Investigation, Formal analysis. **Keith Goulding:** Writing - review & editing. **Fusuo Zhang:** Writing - review & editing. **Xuejun Liu:** Conceptualization, Investigation, Writing - original draft, Supervision, Project administration, Funding acquisition.

Declaration of Competing Interest

The authors declare that they have no known competing financial interests or personal relationships that could have appeared to influence the work reported in this paper.

Acknowledgment

We thank Prof. Peter Vitousek at Stanford University of the United States for his valuable comments on the paper. This work was supported

by the Chinese State Key Research & Development Programme (2017YFC0210100, 2017YFD0200101, 2018YFC0213302, DQGG0208); the National Natural Science Foundation of China (41425007, 41705130), the special contract for science and technology project of Fujian Branch of China Tobacco Corporation (Minyansi Document No. [2014] 2 and Minyan Contract No. (2014) 185), the Deutsche Forschungsgemeinschaft (DFG, German Research Foundation)-328017493/GRK 2366 (Sino-German IRTG AMAIZE-P) and the UK-China Virtual Joint Centre for Improved Nitrogen Agronomy (CINAg).

Appendix A. Supplementary material

Supplementary data to this article can be found online at https://doi.org/10.1016/j.envint.2020.106022.

References

Ackerman, D., Millet, D.B., Chen, X., 2019. Global estimates of inorganic nitrogen deposition across four decades. Global Biogeochem. Cycles 33, 100–107. https://doi.org/10.1029/2018GB005990.

Al-Khashman, O.A., 2005. Study of chemical composition in wet atmospheric precipitation in Eshidiya area. Jordan. Atmos. Environ. 39, 6175–6183. https://doi.org/10.1016/j.atmosenv.2005.06.056.

An, Z., Huang, R.J., Zhang, R., Tie, X., Li, G., Cao, J., Zhou, W., Shi, Z., Han, Y., Gu, Z., 2019. Severe haze in Northern China: a synergy of anthropogenic emissions and atmospheric processes. Proc. Natl. Acad. Sci. U. S. A. 116, 8657–8666. https://doi.org/10.1073/pnas.1900125116.

Backes, A.M., Aulinger, A., Bieser, J., Matthias, V., Quante, M., 2016. Ammonia emissions in Europe, part II: How ammonia emission abatement strategies affect secondary aerosols. Atmos. Environ. 126, 153–161. https://doi.org/10.1016/j.atmosenv.2015.11.039.

Bleeker, Albert, Sutton, Mark A., Acherman, Beat, Alebic-Juretic, Ana, Aneja, Viney P., Ellermann, Thomas, Erisman, Jan Willem, Fowler, David, Fagerli, Hilde, Gauger, Thomas, Harlen, K.S., Hole, Lars Robert, Horvath, Laszlo, Mitosinkova, Marta, Smith, Ron I., Tang, Y. Sim, van Pul, Addo, 2009. In: Atmospheric Ammonia. Springer Netherlands, Dordrecht, pp. 123–180. https://doi.org/10.1007/978-1-4020-9121-6_11.

Bonten,, L.T., Reinds,, G.J., Posch, M., 2016. A model to calculate effects of atmospheric deposition on soil acidification, eutrophication and carbon sequestration. Environ. Modell Softw. 79, 75–84. https://doi.org/10.1016/j.envsoft.2016.01.009.

Chen, H., Kwong, J.C., Copes, R., Hystad, P., van Donkelaar, A., Tu, K., Brook, J.R., Goldberg, M.S., Martin, R.V., Murray, B.J., Wilton, A.S., Kopp, A., Burnett, R.T., 2017. Exposure to ambient air pollution and the incidence of dementia: a populationbased cohort study. Environ. Int. 108, 271–277. https://doi.org/10.1016/j.envint.2017.08.020.

Chen, S., Cheng, M., Guo, Z., Xu, W., Du, X., Li, Y., 2020. Enhanced atmospheric NH_3 pollution in China from 2008 to 2016: evidence from a combination of observations and emissions. Environ. Pollut. 114421. https://doi.org/10.1016/j.envpol.2020.114421.

Crippa, M., Solazzo, E., Huang, G., Guizzardi, D., Koffi, E., Muntean, M., Schieberle, C., Friedrich, R., Janssens-Maenhout, G., 2020. High resolution temporal profiles in the Emissions Database for Global Atmospheric Research. Sci. Data 7, 1–17. https://doi.org/10.1038/s41597-020-0462-2.

Cui, Y., Lin, J., Song, C., Liu, M., Yan, Y., Xu, Y., Huang, B., 2016. Rapid growth in nitrogen dioxide pollution over Western China, 2005–2013. Atmos. Chem. Phys. 16, 6207–6221. https://doi.org/10.5194/acp-16-6207-2016.

Du, E., De Vries, W., Galloway, J.N., Hu, X., Fang, J., 2014. Changes in wet nitrogen deposition in the United States between 1985 and 2012. Environ. Res. Lett. 9, 1–9. https://doi.org/10.1088/1748-9326/9/9/095004.

Duan, L., Liu, J., Xin, Y., Larssen, T., 2013. Air-pollution emission control in China: impacts on soil acidification recovery and constraints due to drought. Sci. Total Environ. 463, 1031–1041. https://doi.org/10.1016/j.scitotenv.2013.06.108.

Fowler, D., Duyzer, J., Baldocchi, D., 1990. Inputs of trace gases, particles and cloud droplets to terrestrial surfaces. Proc. Royal Soc. Edinburgh Sect. B: Biol. Sci. 97, 35–59. https://doi.org/10.1017/S0269727000005285.

Galloway, J.N., Dentener, F.J., Capone, D.G., Boyer, E.W., Howarth, R.W., Seitzinger, S.P., Asner, G.P., Cleveland, C.C., Green, P.A., Holland, E.A., Karl, D.M., Michaels, A.F., Porter, J.H., Townsend, A.R., Vorosmarty, C.J., 2004. Nitrogen cycles: past, present, and future. Biogeochemistry 70, 153–226. https://doi.org/10.1007/s10533-004-0370-0.

Galloway, J.N., Townsend, A.R., Erisman, J.W., Bekunda, M., Cai, Z., Freney, J.R., Martinelli, L.A., Seitzinger, S.P., Sutton, M.A., 2008. Transformation of the nitrogen cycle: recent trends, questions, and potential solutions. Science 320, 889–892. https://doi.org/10.1126/science.1136674.

Gupta, A., Kumar, R., Kumari, K.M., Srivastava, S., 2003. Measurement of NO_2, HNO_3, NH_3 and SO_2 and related particulate matter at a rural site in Rampur. India. Atmos. Environ. 37, 4837–4846. https://doi.org/10.1016/j.atmosenv.2003.07.008.

Hou, Y., Velthof, G.L., Oenema, O., 2015. Mitigation of ammonia, nitrous oxide and methane emissions from manure management chains: a meta-analysis and integrated assessment. Glob. Change Biol. 21, 1293–1312. https://doi.org/10.1111/gcb.12767.

Huang, C., Hu, Q., Lou, S., Tian, J., Wang, R., Xu, C., An, J., Ren, H., Ma, D., Quan, Y., 2018. Ammonia emission measurements for light-duty gasoline vehicles in china and implications for emission modeling. Environ. Sci. Technol. 52, 11223–11231. https://doi.org/10.1021/acs.est.8b03984.

Huang, R.J., Zhang, Y.L., Bozzetti, C., Ho, K.F., Cao, J.J., Han, Y.M., Daellenbach, K.R., Slowik, J.G., Platt, S.M., Canonaco, F., Zotter, P., Wolf, R., Pieber, S.M., Bruns, E.A., Crippa, M., Ciarelli, G., Piazzalunga, A., Schwikowski, M., Abbaszade, G., Schnelle-Kreis, J., Zimmermann, R., An, Z.S., Szidat, S., Baltensperger, U., El Haddad, I., Prevot, A.S.H., 2014. High secondary aerosol contribution to particulate pollution during haze events in China. Nature 514, 218–222. https://doi.org/10.1038/nature13774.

Huang, X., Song, Y., Li, M., Li, J., Huo, Q., Cai, X., Zhu, T., Hu, M., Zhang, H., 2012. A high-resolution ammonia emission inventory in China. Global Biogeochem. Cycles 26, 1–14. https://doi.org/10.1029/2011GB004161.

Johnson, J., Graf Pannatier, E., Carnicelli, S., Cecchini, G., Clarke, N., Cools, N., Hansen, K., Meesenburg, H., Nieminen, T.M., Pihl-Karlsson, G., 2018. The response of soil solution chemistry in European forests to decreasing acid deposition. Glob. Change Biol. 24, 3603–3619. https://doi.org/10.1111/gcb.14156.

Kang, Y.N., Liu, M.X., Song, Y., Huang, X., Yao, H., Cai, X.H., Zhang, H.S., Kang, L., Liu, X.J., Yan, X.Y., He, H., Zhang, Q., Shao, M., Zhu, T., 2016. High-resolution ammonia emissions inventories in China from 1980 to 2012. Atmos. Chem. Phys. 16, 2043–2058. https://doi.org/10.5194/acp-16-2043-2016.

Lachatre, M., Fortems-Cheiney, A., Foret, G., Siour, G., Dufour, G., Clarisse, L., Clerbaux, C., Coheur, P.-F., Damme, M.V., Beekmann, M., 2019. The unintended consequence of SO_2 and NO_2 regulations over China: increase of ammonia levels and impact on $PM_{2.5}$ concentrations. Atmos. Chem. Phys. 19, 6701–6716. https://doi.org/10.5194/acp-2018-1092.

Li, Y., Schichtel, B.A., Walker, J.T., Schwede, D.B., Chen, X., Lehmann, C.M., Puchalski, M.A., Gay, D.A., Collett, J.L., 2016. Increasing importance of deposition of reduced nitrogen in the United States. Proc. Natl. Acad. Sci. U. S. A. 113, 5874–5879. https://doi.org/10.1073/pnas.1525736113.

Liu, L., Zhang, X., Xu, W., Liu, X., Li, Y., Lu, X., Zhang, Y., Zhang, W., 2017. Temporal characteristics of atmospheric ammonia and nitrogen dioxide over China based on emission data, satellite observations and atmospheric transport modeling since 1980. Atmos. Chem. Phys. 17, 9365–9378. https://doi.org/10.5194/acp-17-9365-2017.

Liu, M., Huang, X., Song, Y., Tang, J., Cao, J., Zhang, X., Zhang, Q., Wang, S., Xu, T., Kang, L., 2019. Ammonia emission control in China would mitigate haze pollution and nitrogen deposition, but worsen acid rain. Proc. Natl. Acad. Sci. U. S. A. 116, 7760–7765. https://doi.org/10.1073/pnas.1814880116.

Liu, X.J., Xu, W., Sha, Z.P., Zhang, Y.Y., Wen, Z., Wang, J.X., Zhang, F.S., Goulding, Keith, 2020. A green eco-environment for sustainable development: framework and action. Front. Agr. Sci. Eng. 7, 67–74. https://doi.org/10.15302/J-FASE-2019297.

Liu, X.J., Zhang, Y., Han, W.X., Tang, A.H., Shen, J.L., Cui, Z.L., Vitousek, P., Erisman, J.W., Goulding, K., Christie, P., Fangmeier, A., Zhang, F.S., 2013. Enhanced nitrogen deposition over China. Nature 494, 459–462. https://doi.org/10.1038/nature11917.

Lu, X., Mao, Q., Gilliam, F.S., Luo, Y., Mo, J., 2014. Nitrogen deposition contributes to soil acidification in tropical ecosystems. Glob. Change Biol. 20, 3790–3801. https://doi.org/10.1111/gcb.12665.

Meng, W., Zhong, Q., Yun, X., Zhu, X., Huang, T., Shen, H., Chen, Y., Chen, H., Zhou, F., Liu, J., 2017. Improvement of a global high-resolution ammonia emission inventory for combustion and industrial sources with new data from the residential and transportation sectors. Environ. Sci. Technol. 51, 2821–2829. https://doi.org/10.1021/acs.est.6b03694.

Midolo, G., Alkemade, R., Schipper, A.M., Benítez-López, A., Perring, M.P., De Vries, W., 2019. Impacts of nitrogen addition on plant species richness and abundance: a global meta-analysis. Global Ecol. Biogeography 28, 398–413. https://doi.org/10.1111/geb.12856.

Nair, R.K., Perks, M.P., Weatherall, A., Baggs, E.M., Mencuccini, M., 2016. Does canopy nitrogen uptake enhance carbon sequestration by trees? Glob. Change Biol. 22, 875–888. https://doi.org/10.1111/gcb.13096.

Ohara, T., Akimoto, H., Kurokawa, J.-I., Horii, N., Yamaji, K., Yan, X., Hayasaka, T., 2007. An Asian emission inventory of anthropogenic emission sources for the period 1980–2020. Atmos. Chem. Phys. 7, 4419–4444. https://doi.org/10.5194/acp-7-4419-2007.

Oulehle, F., Evans, C.D., Hofmeister, J., Krejci, R., Tahovska, K., Persson, T., Cudlin, P., Hruska, J., 2011. Major changes in forest carbon and nitrogen cycling caused by declining sulphur deposition. Glob. Change Biol. 17, 3115–3129. https://doi.org/10.1111/j.1365-2486.2011.02468.x.

Pan, Y., Tian, S., Liu, D., Fang, Y., Zhu, X., Zhang, Q., Zheng, B., Michalski, G., Wang, Y., 2016. Fossil fuel combustion-related emissions dominate atmospheric ammonia sources during severe haze episodes: evidence from ^{15}N-stable isotope in size-resolved aerosol ammonium. Environ. Sci. Technol. 50, 8049–8056. https://doi.org/10.1021/acs.est.6b00634.

Pan, Y., Wang, Y., Tang, G., Wu, D., 2012. Wet and dry deposition of atmospheric nitrogen at ten sites in Northern China. Atmos. Chem. Phys. 2, 6515–6535. https://doi.org/10.5194/acp-12-6515-2012.

Schmitz, A., Sanders, T.G., Bolte, A., Bussotti, F., Dirnböck, T., Johnson, J., Penuelas, J., Pollastrini, M., Prescher, A.K., Sardans, J., 2018. Responses of forest ecosystems in Europe to decreasing nitrogen deposition. Environ. Pollut. 244, 980–994. https://doi.org/10.1016/j.envpol.2018.09.101.

Sha, Z., Ma, X., Loick, N., Lv, T., Cardenas, L.M., Ma, Y., Liu, X., Misselbrook, T., 2020. Nitrogen stabilizers mitigate reactive N and greenhouse gas emissions from an arable soil in North China Plain: field and laboratory investigation. J. Clean Prod. 121025. https://doi.org/10.1016/j.jclepro.2020.121025.

Sutton, M.A., Asman, W.A., Ellermann, T., Van Jaarsveld, J., Acker, K., Aneja, V., Duyzer,

J., Horvath, L., Paramonov, S., Mitosinkova, M., 2003. Establishing the link between ammonia emission control and measurements of reduced nitrogen concentrations and deposition. Environ. Monit. Assess. 82, 149–185. https://doi.org/10.1023/A:1021834132138.

Tan, J., Fu, J.S., Dentener, F., Sun, J., Emmons, L., Tilmes, S., Flemming, J., Takemura, T., Bian, H., Zhu, Q., 2018. Source contributions to sulfur and nitrogen deposition–an HTAP II multi-model study on hemispheric transport. Atmos. Chem. Phys. 18, 12223–12240. https://doi.org/10.5194/acp-18-12223-2018.

Vet, Robert, Artz, Richard S., Carou, Silvina, Shaw, Mike, Ro, Chul-Un, Aas, Wenche, Baker, Alex, Bowersox, Van C., Dentener, Frank, Galy-Lacaux, Corinne, Hou, Amy, Pienaar, Jacobus J., Gillett, Robert, Forti, M. Cristina, Gromov, Sergey, Hara, Hiroshi, Khodzher, Tamara, Mahowald, Natalie M., Nickovic, Slobodan, Rao, P.S.P., Reid, Neville W., 2014. A global assessment of precipitation chemistry and deposition of sulfur, nitrogen, sea salt, base cations, organic acids, acidity and pH, and phosphorus. Atmos. Environ. 93, 3–100. https://doi.org/10.1016/j.atmosenv.2013.10.060.

Warner, J.X., Wei, Z., Strow, L.L., Dickerson, R.R., Nowak, J.B., 2016. The global tropospheric ammonia distribution as seen in the 13-year AIRS measurement record. Atmos. Chem. Phys. 16, 5467. https://doi.org/10.5194/acp-16-5467-2016.

Xu, D., Ge, B., Wang, Z., Sun, Y., Chen, Y., Ji, D., Yang, T., Ma, Z., Cheng, N., Hao, J., 2017. Below-cloud wet scavenging of soluble inorganic ions by rain in Beijing during the summer of 2014. Environ. Pollut. 230, 963–973. https://doi.org/10.1016/j.envpol.2017.07.033.

Xu, W., Luo, X.S., Pan, Y.P., Zhang, L., Tang, A.H., Shen, J.L., Zhang, Y., Li, K.H., Wu, Q.H., Yang, D.W., Zhang, Y.Y., Xue, J., Li, W.Q., Li, Q.Q., Tang, L., Lu, S.H., Liang, T., Tong, Y.A., Liu, P., Zhang, Q., Xiong, Z.Q., Shi, X.J., Wu, L.H., Shi, W.Q., Tian, K., Zhong, X.H., Shi, K., Tang, Q.Y., Zhang, L.J., Huang, J.L., He, C.E., Kuang, F.H., Zhu, B., Liu, H., Jin, X., Xin, Y.J., Shi, X.K., Du, E.Z., Dore, A.J., Tang, S., Collett, J.L., Goulding, K., Sun, Y.X., Ren, J., Zhang, F.S., Liu, X.J., 2015. Quantifying atmospheric nitrogen deposition through a nationwide monitoring network across China. Atmos. Chem. Phys. 15, 12345–12360. https://doi.org/10.5194/acp-15-12345-2015.

Xu, W., Zhang, L., Liu, X., 2019a. A database of atmospheric nitrogen concentration and deposition from the nationwide monitoring network in China. Sci. Data 6, 51. https://doi.org/10.1038/s41597-019-0061-2.

Xu, W., Zheng, K., Liu, X., Meng, L., Huaitalla, R.M., Shen, J., Hartung, E., Gallmann, E., Roelcke, M., Zhang, F., 2014. Atmospheric NH3 dynamics at a typical pig farm in China and their implications. Atmos. Pollut. Res. 5, 455–463. https://doi.org/10.5094/APR.2014.053.

Xu, Z., Liu, M., Zhang, M., Song, Y., Wang, S., Zhang, L., Xu, T., Wang, T., Yan, C., Zhou, T., 2019b. High efficiency of livestock ammonia emission controls in alleviating particulate nitrate during a severe winter haze episode in northern China. Atmos. Chem. Phys. 19, 5605–5613. https://doi.org/10.5194/acp-19-5605-2019.

Yang, F., Tan, J., Zhao, Q., Du, Z., He, K., Ma, Y., Duan, F., Chen, G., 2011. Characteristics of $PM_{2.5}$ speciation in representative megacities and across China. Atmos. Chem. Phys. 11, 5207–5219. https://doi.org/10.5194/acp-11-5207-2011.

Yu, G., Jia, Y., He, N., Zhu, J., Chen, Z., Wang, Q., Piao, S., Liu, X., He, H., Guo, X., 2019. Stabilization of atmospheric nitrogen deposition in China over the past decade. Nat. Geosci. 12, 424. https://doi.org/10.1038/s41561-019-0352-4.

Zhan, X., Bo, Y., Zhou, F., Liu, X., Paerl, H.W., Shen, J., Wang, R., Li, F., Tao, S., Dong, Y., 2017. Evidence for the importance of atmospheric nitrogen deposition to eutrophic lake Dianchi, China. Environ. Sci. Technol. 51, 6699–6708. https://doi.org/10.1021/acs.est.6b06135.

Zhang, X., Fang, Q., Zhang, T., Ma, W., Velthof, G.L., Hou, Y., Oenema, O., Zhang, F., 2019. Benefits and trade-offs of replacing synthetic fertilizers by animal manures in crop production in China: a meta-analysis. Glob. Change Biol. 26, 888–900. https://doi.org/10.1111/gcb.14826.

Zhang, X.M., Wu, Y.Y., Liu, X.J., Reis, S., Jin, J.X., Dragosits, U., Van Damme, M., Clarisse, L., Whitburn, S., Coheur, P.F., Gu, B.J., 2017. Ammonia emissions may be substantially underestimated in China. Environ. Sci. Technol. 51, 12089–12096. https://doi.org/10.1021/acs.est.7b02171.

Zhang, Y.Y., Benedict, K., Tang, A.H., Sun, Y.L., Fang, Y.T., Liu, X.J., 2020. Persistent non-agricultural and periodic agricultural emissions dominate sources of ammonia in urban Beijing: evidence from ^{15}N stable isotope in vertical profiles. Environ. Sci. Technol. 54, 102–109. https://doi.org/10.1021/acs.est.9b05741.

Zhao, Y., Zhang, L., Chen, Y., Liu, X., Xu, W., Pan, Y., Duan, L., 2017. Atmospheric nitrogen deposition to China: a model analysis on nitrogen budget and critical load exceedance. Atmos. Environ. 153, 32–40. https://doi.org/10.1016/j.atmosenv.2017.01.018.

Zheng, B., Tong, D., Li, M., Liu, F., Hong, C., Geng, G., Li, H., Li, X., Peng, L., Qi, J., 2018. Trends in China's anthropogenic emissions since 2010 as the consequence of clean air actions. Atmos. Chem. Phys. 18, 14095–14111. https://doi.org/10.5194/acp-18-14095-2018.